JOURNAL SOLID STATE CHEMISTRY

ACCEPTED MANUSCRIPT

$(Pt_{1-x}Cu_x)_3Cu_2B$ and $Pt_9Cu_3B_5$, the First Examples of Copper Platinum Borides. Observation of Superconductivity in a Novel Boron Filled β-Mn-type compound.

Leonid P. Salamakha[1], Oksana Sologub[1,*], Berthold Stöger[2], Herwig Michor[1], Ernst Bauer[1], Peter F. Rogl[3]

[1]Institute of Solid State Physics, Vienna University of Technology, A-1040 Wien, Austria

[2]Institute for Chemical Technologies and Analytics, Vienna University of Technology, A-1040 Wien, Austria

[3]Institute of Physical Chemistry, University of Vienna, A-1090 Wien, Austria

ABSTRACT

New ternary copper platinum borides have been synthesized by arc melting of pure elements followed by annealing at 600 °C. The structures have been studied by X-ray single crystal and powder diffraction. $(Pt_{1-x}Cu_x)_3Cu_2B$ (x=0.33) forms a B-filled β-Mn-type structure (space group $P4_132$; a=0.6671(1) nm). Cu atoms are distributed preferentially on the 8*c* atom sites, whereas the 12*d* site is randomly occupied by Pt and Cu atoms (0.670(4) Pt/0.330(4) Cu). Boron is located in octahedral voids of the parent β-Mn-type structure. $Pt_9Cu_3B_5$ (space group *P*-62*m*; a=0.9048(3) nm, c=0.2908(1) nm) adopts the $Pt_9Zn_3B_{5-\delta}$-type structure. It has a columnar architecture along the short translation vector exhibiting three kinds of $[Pt_6]$ trigonal prism columns (boron filled, boron semi-filled and empty) and Pt channels with a pentagonal cross section filled with Cu atoms. The striking structural feature is a $[Pt_6]$ cluster in form of an empty trigonal prism at the origin of the unit cell, which is surrounded by

coupled [BPt_6] and [Pt_6] trigonal prisms, rotated perpendicularly to the central one. There is no B-B contact as well as Cu-B contact in the structure. The relationships of $Pt_9Cu_3B_5$ structure with the structure of $Ti_{1+x}Os_{2-x}RuB_2$ as well as with the structure families of metal sulfides and aluminides have been elucidated.

$(Pt_{1-x}Cu_x)_3Cu_2B$ (x=0.3) (B-filled β-Mn-type structure) is a bulk superconductor with a transition temperature of about 2.06 K and an upper critical field $\mu_0H_{C2}(0)^{WHH}$ of 1.2 T, whereas no superconducting transition has been observed up to 0.3 K in $Pt_9Cu_3B_5$ ($Pt_9Zn_3B_{5-\delta}$-type structure) from electrical resistivity measurements.

Keywords: Copper Platinum Borides; Crystal Structure; Electrical Transport Properties

* Corresponding author

E-mail address: oksana.sologub@univie.ac.at.

1. **Introduction**

Structure, phase transitions and chemical bonding in TM'-TM-B ternary systems (TM',TM - transition metals) are subjects of intense investigations for the past decades due to the technological importance of these alloys arising from high temperature, mechanical, electrical and magnetic properties. A growing interest in the borides of the 4^{th} -10^{th} groups such as so-called "Mo_2FeB_2 complex boride base hard alloys" including constituent binary borides [1-3], ReB_2 as one of the hardest metal-based materials [4], superconducting MgB_2 [5], stimulated the development and application of a range of advanced compound prediction computing methods [6,7] which led to new outstanding discoveries, e.g. superconducting FeB_4 (at 2.9 K) and super-hard γB_{28}. While binary TM borides in general are continuously under broad scrutiny [8] the studies of TM'-TM-B ternary systems are limited to several research groups [9,10]. Lately, a substantial body of experimental and theoretical studies is devoted to ternary and quaternary transition metal-rich borides containing a magnetically active element [9,11-13]; these investigations resulted in a number of significant reports, e.g. i) identification of a new twofold superstructure of U_3Si_2 in Nb_2OsB_2, and Zr_2Ir_6B with an eightfold superstructure of the cubic perovskite-like boride $ZrIr_3B_{0.5}$ [14,15]; ii) first observation of trigonal-planar B_4-units [16], *etc*. Our recent work on Fe(Co)-Ir-B compounds led us to experimental observation of boron-rich tau-borides with a non-centrosymmetric structure exhibiting a novel structural unit of boron atoms, boron tetrahedra [B_4] [17]. In continuation of this work, we turned our attention to the ternary platinum boride systems with copper for which hitherto no information on compound formation exists in the literature. As a consequence, two new ternary borides of the Cu-Pt-B family have been observed, i.e. the ternary compound of filled β-Mn-type structure and the compound $Pt_9Cu_3B_5$ forming a fully ordered structure related to $Ti_{1+x}Os_{2-x}RuB_2$.

Elemental β-Mn exhibits a cubic structure: space group $P4_132$ (no. 213) a = 0.6304 nm, Mn2 in 12d (⅛,y,y+¼); Mn1 in 8c (x,x,x), Z=20 [18]. Mn1 is in icosahedral coordination and the coordination polyhedron of Mn2 is a highly distorted CN14 polyhedron which occurs in tetrahedrally close-packed structures. Several descriptions of this structure type are given in the literature [19-23] serving to put emphasis on different aspects of the β-Mn structure. Very recently a relation was given tracing the β-Mn structure to the cubic Laves phase $MgCu_2$ [24]. The octahedral voids of β-Mn can be occupied by atoms of light elements (B, C, N); the first filled β-Mn structure was observed in Mo_3Al_2C [25]. Filled β-Mn type compounds attract attention due to the possibility to exhibit an unconventional superconducting state: Mo_3Al_2C was reported [26] to exhibit a superconducting transition at rather high temperature of 9 K and upper critical field $\mu_0 H_{C2}$ of 15.7 T [27,28]. In recent work Bauer et al. (2014) [29] proved the absence of time-reversal symmetry breaking in this compound despite its non-centrosymmetric crystal structure. Among the compounds with boron, only few were found to adopt the β-Mn structure; all of them were reported to exhibit superconductivity at low temperatures, i.e. i) Li_2Pd_3B and Li_2Pt_3B show superconducting transitions at 7 K and 2 K, respectively [30,31,32]; ii) $W_7Re_{13}B$ and $Mo_7Re_{13}B$ are superconductors with T_c's of 7.1 and 8.3 K, respectively [33]; iii) a superconducting transition in Cr_2Re_3B occurs at 4.8 K [34].

Ternary boride systems with platinum constitute a particular case in the chemistry of borides. Not mentioning the binary boundary Pt-B which appeared to be not studied completely [35], only few ternary rare earth-platinum boride series have been reported so far [36-38] in comparison with, e.g., the multitude of studies presented for the ternary rare earth boride systems with rhodium or iridium. The investigations of Ce(Eu,Yb)-Pt-B systems are underway revealing extreme complexity of ternary phase diagrams and crystal structures of compounds [35-38]. Furthermore, in contrast to the Ir-Zn-B family [39,40] which exhibits

rich structural chemistry, only one compound has hitherto been found in Pt-Zn-B system [41] and no data exist in the literature on the interaction of platinum with copper and boron. Thus, in the work given herein we focus on i) the synthesis and structural studies of the two novel ternary compounds in the Pt-Cu-B system; ii) structural relationships for $(Pt_{1-x}Cu_x)_3Cu_2B$ and analysis of site preferences; iii) interpretation of the $Pt_9Cu_3B_5$ structure in the view of recently discovered $Ti_{1+x}Os_{2-x}RuB_2$ [42,43], widely recognized for the first observation of a new boron trigonal-planar B_4 structural unit, as well as in comparison with aluminide and chalcogenide structures; iv) electrical transport properties down to 0.3 K for both compounds including the evaluation of upper critical field of the new superconductor $(Pt_{1-x}Cu_x)_3Cu_2B$. Further experiments on the elucidation of the superconducting state of $(Pt_{1-x}Cu_x)_3Cu_2B$, such as low temperature specific heat and magnetic susceptibility measurements, as well as on the exploration of the isothermal section of the Pt-Cu-B system at 600 ºC are in progress and will be subjects of our forthcoming paper.

2. Experimental

2.1. Synthesis and phase analysis

Alloys were prepared from ingots of thoroughly re-melted pieces of platinum sponge (Ögussa, Austria, 99.99 mass%), Cu shot (2-6mm, 99.999 mass%, ChemPur, Germany) and crystalline boron (ChemPur, Germany, 99.4 mass%) by repeated arc melting under argon. The arc-melted buttons were wrapped in tantalum foil and vacuum-sealed in a quartz tube for annealing at 600 °C for 240 hours. Lattice parameters and standard deviations were determined by least square refinements of room temperature X-ray powder diffraction (XRD) data obtained from a Guinier-Huber image plate employing monochromatic $CuK_{\alpha 1}$ radiation (or alternatively $FeK_{\alpha 1}$ radiation) and Ge as internal standard (a_{Ge}=0.565791 nm). XRD Rietveld refinements were performed with the program FULLPROF [44] with the use of its internal tables for atom scattering factors. For quantitative analysis of the Pt/Cu ratio, the

annealed samples were polished using standard procedures and were examined by scanning electron microscopy (SEM).

2.2. Structural X-ray diffraction studies

The crystal structures of compounds were elucidated from X-ray diffraction intensity data of single crystals which were isolated via mechanical fragmentation of the annealed $Pt_{37}Cu_{46.3}B_{16.7}$ and $Pt_{53}Cu_{18}B_{29}$ samples. The crystals were measured on a four-circle Bruker APEX II diffractometer equipped with a CCD detector (κ-geometry, Mo Kα radiation); orientation matrices and unit cell parameters were derived using the APEX II software [45]. Multi-scan absorption correction was applied using the program SADABS; frame data were reduced to intensity values applying the SAINT-Plus package [46]. The structures were solved by direct methods and refined with the SHELXS-97 and SHELXL-97 programs [47,48], respectively. Further details concerning the experiments are summarized in Table 1.

2.3. Electrical resistivity

Electrical resistivity of the compounds described above was studied using an a.c. bridge (Lakeshore) in the range from room temperature down to 0.3 K.

3. Results and discussions

3.1. Crystal structure refinements

$(Pt_{1-x}Cu_x)_3Cu_2B$ (x=0.33). X-ray single crystal diffraction data were completely indexed in a cubic primitive lattice (a=0.6671(1) nm). The statistical intensity distribution tests [50] of diffraction data ($|E^2-1|$ = 0.555) hinted at high probability of a non-centrosymmetricity of the structure. Inspection of the systematically absent reflections (WinGX program package [51]) revealed the Laue class m-3m and extinction symbol $P4_1$--, thus leading to the enantiomorphic pair of space groups $P4_132$ (no. 213) and $P4_332$ (no. 212) of which the first one was confirmed to be correct by subsequent successful structure solution

and refinement against F^2 values. Structure solution by direct methods resulted in two atom positions, one of which (12*d*) was assigned to Pt and another one (8*c*) to Cu. Boron was found on a 4*a* site from the analysis of the electron density peaks in difference Fourier maps. The obtained structure model corresponds to that reported for the filled *β*-Mn structure, Mo_3Al_2C [25], where Mo and Al atoms occupy the atom positions of Mn in an ordered way while C is located in octahedral voids. The 12*d* site occupied by Pt exhibits significantly large displacement parameters suggesting a possible site-sharing by platinum and copper. A mixed occupancy refinement resulted in 0.670(4) Pt+0.330(4) Cu in Wyckoff site 12*d*, while no platinum could be refined in the 8*c* site. The composition was confirmed by SEM-measurements, giving a Pt:Cu ratio of 1:1.25. Anisotropic displacement parameters were used only for the metal atoms, while boron was refined isotropically. Final refinement yielded a reliability factor as low as R_F^2=0.0157 and no significant residual electron density peaks (+1.30/-1.04 e-/Å^3). The relevant crystallographic data are given in Table 1; for bond lengths values see Table 2.

X-ray powder diffraction intensities collected from the polycrystalline alloy with nominal composition $Pt_{36}Cu_{47.3}B_{16.7}$ were in good agreement with the intensities calculated from the structural model obtained from the single crystal as inferred from Rietveld refinement (Supporting information, Fig. 1).

In order to explore the possibility of Pt/Cu atom ordering, the refinement from single crystal X-ray diffraction data has been carried out in the maximal non-isomorphic subgroup *R*32 ($P4_132 \rightarrow t4 \rightarrow R32$, no. 155) (applying the transformation matrix (*a*-*b*, *b*-*c*, *a*+*b*+*c*) for direct cell axes and *hkl*). Despite the symmetry reduction offered an increased flexibility for the structure due to a split of the Wyckoff positions of Pt/Cu, Cu and B into several symmetry-independent positions (i.e. *18*- and two *9*-fold for Pt/Cu, *18*- and *6*-fold for Cu and *9*- and *3*-fold for B), the structural characteristics were found to be identical in both models.

The refinement of occupancy parameters resulted in equal values for all three new disordered Pt/Cu atom sites, however, revealing a slightly higher total Pt population (0.700(3)Pt/0.300(3)Cu) than in the initial cubic structure model. A check on missing symmetry via the program PLATON [51] suggested the afore-derived cubic solution definitely indicating no essential deviations of the atom positions from the higher symmetry locations thus triggering the conclusion that the structure of the crystal investigated is consistent with the structure model obtained in the space group $P4_132$.

$Pt_9Cu_3B_5$. The isotypy of this compound with the corresponding platinum zinc boride [41] could already be assumed from the X-ray powder diffraction pattern. Consequently, careful examination of the single crystal X-ray diffraction data set showed that the systematic extinctions were compatible with space group *P*-62*m*. Structure solution with direct methods led to three metal atom positions, which were assigned to two platinum (6*k* and 3*f*) and one copper (3*f*) atoms. Subsequent difference Fourier syntheses revealed two atom positions of boron (3*g* and 2*c*) thus leading to a composition $Pt_9Cu_3B_5$ with one formula unit per unit cell. The structure was refined with anisotropic atomic displacement parameters for platinum and copper atoms and isotropic displacement parameters for the light boron atoms. Since the structure refinement of the prototype structure $Pt_9Zn_3B_{5-\delta}$ revealed significant defects on the B2 site (2*c* ⅓,⅔,0; Oc. 0.5), also the occupancy parameters of atoms in the $Pt_9Cu_3B_5$ crystal were refined in separate series of least-squares cycles. This procedure revealed no defects for any atom site, leading to a stoichiometric composition $Pt_9Cu_3B_5$ for the crystal investigated. The final difference Fourier synthesis was flat; the positional parameters and interatomic distances are listed in Table 1 and in Table 2, respectively. The structure model obtained from the single crystal was confirmed by Rietveld analysis of the X-ray powder data exhibiting low residual values and good agreement between calculated and observed

intensities (a=0.90577(2) nm, c=0.291038(6) nm, $R_F=\Sigma|F_o-F_c|/\Sigma F_o=0.028$, $R_I=\Sigma|I_o-I_c|/\Sigma I_o=0.043$).

Crystallographic data in CIF format have also been deposited with Fachinformationszentrum Karlsruhe, 76344 Eggenstein-Leopoldshafen, Germany, (fax: (49) 7247-808-666; e-mail: crysdata@fiz.karlsruhe.de) with depository numbers CSD- 429501 for $(Pt_{1-x}Cu_x)_3Cu_2B$ (x=0.33) and CSD- 429502 for $Pt_9Cu_3B_5$.

3.2. Description of the crystal structures

$(Pt_{1-x}Cu_x)_3Cu_2B$ (x=0.33). The characteristic building elements of $(Pt_{1-x}Cu_x)_3Cu_2B$ are distorted 0.67Pt/0.33Cu octahedra (in further description denoted as Pt/Cu) centered by boron atoms. The octahedra interlink via common corners and form a three-dimensional framework exhibiting large cages around the Wyckoff site 8*c* occupied by Cu atoms. Fig. 1a portrays the crystal structure of $(Pt_{1-x}Cu_x)_3Cu_2B$ in three-dimensional view along [001] emphasizing the coordination polyhedra for boron. All the bond lengths between the central boron and Pt/Cu atoms at vertices are uniformly equal 0.21157(3) nm. Every copper in 8*c* is surrounded by 9 Pt/Cu and 3 Cu forming a distorted icosahedron. Pt/Cu resides in a 14-vertices polyhedron and is bonded to 2 boron atoms ($d_{Pt/Cu-B}$=0.2116 nm), 6 Cu ($d_{Pt/Cu-Cu}$=0.2729 nm – 0.2801 nm) and 6 Pt/Cu ($d_{Pt/Cu-Pt/Cu}$=0.27267 nm and 0.29983 nm). Coordination polyhedra of Cu and Pt/Cu are given in Fig. 1b-c. Copper atoms build a three dimensional network in which each Cu is linked to three adjacent copper atoms; the Cu sub-lattice interpenetrates through the interstices within the octahedral $[B(Pt/Cu)_6]$ framework (Fig. 1d).

$Pt_9Cu_3B_5$. The columnar structure of $Pt_9Cu_3B_5$ is built up of intricate connectivity of two kinds of $[BPt_6]$ trigonal prisms with non-parallel prism axes which share bases ($[B2Pt_6]$, prism's axes coincide with *c* direction) and edges ($[B1Pt_6]$, lying perpendicular to $[B2Pt_6]$) to form distinct columns running along *z*; in the columns built by $[B1Pt_6]$, every second prism is empty (Fig. 2e). The columns interlink in the *ab* plane through the edges of trigonal prisms;

Table 1. X-ray single crystal structure data[a)]

Parameter/Compound	$(Pt_{1-x}Cu_x)_3Cu_2B$, x=0.33	$Pt_9Cu_3B_5$
Nominal composition	$Pt_{33.5}Cu_{49.8}B_{16.7}$	$Pt_{52.9}Cu_{17.7}B_{29.4}$
Space group	$P4_132$; No. 213	P-62m; No. 189
Structure type	B-filled β-Mn, disordered Mo_3Al_2C	$Pt_9Zn_3B_{5-\delta}$
Formula from refinement	$Pt_{2.01}Cu_{2.99}B$; $(Pt_{1-x}Cu_x)_3Cu_2B$ (x=0.33)	$Pt_9Cu_3B_5$
Range for data collection	$4.32°<\theta<29.61°$	$2.60°<\theta<32.63°$
Crystal size	$43x40x40\mu m^3$	$0.40\times37\times30\ \mu m^3$
a [nm]	0.66706(11)	0.9048(3)
c [nm]		0.29085(10)
Reflections in refinement	125 $F_o>4\sigma(F_o)$ of 191	319 $F_o>4\sigma(F_o)$ of 1837
Mosaicity	<0.4	<0.4
Number of variables	12	18
$R_F^2=\Sigma\lvert F_0^2-F_c^2\rvert/\Sigma F_0^2$	0.0157	0.0337
Flack parameter	0.02(5)	-0.01(8)
GOF	1.191	0.658
Extinction (Zachariasen)	0.0013(4)	0.0020(6)
M1; occ.; U_{11}[b], U_{22}, U_{33}, U_{23}, U_{13}, U_{12}	12d (⅛,y,y+¼) y=0.1915[d],z=0.4415[d]; 0.670(4) Pt+0.330(4) Cu; 0.147(3), $U_{22}=U_{33}$=0.134(2), 0.018(2), 0.024(1), -0.024(1)	6k (x,y,½) x=0.2635(1), y=0.4603(1) 1.00 Pt1 0.046(5), 0.038(5), 0.075(4), $U_{23}=U_{13}$=0, 0.018(3)
M2; occ.; U_{11}, U_{22}, U_{33}, U_{23}, U_{13}, U_{12}	8c (x,x,x), x=0.0576(1); 1.00 Cu1; $U_{11}=U_{22}=U_{33}$=0.127(4), $U_{23}=U_{13}=U_{12}$=-0.001(4)	3f (x,0,0) x=0.1761[d]; 1.00 Pt2 0.052(5), 0.057(6), 0.082(6), $U_{23}=U_{13}$= 0, 0.028(3)
M3; occ.; U_{11}, U_{22}, U_{33}, U_{23}, U_{13}, U_{12}		3f (x,0,0) x=0.4577(5); 1.00 Cu1 0.068(16), 0.106(22), 0.114(20), $U_{23}=U_{13}$=0, 0.053(11)
B1; occ.; U_{iso}[c]	4a (⅜,⅜,⅜); 1.00 B1; U_{iso}=0.22(5)	3g (x,0, ½) x=0.804(4); 1.00 B1; 0.024(49)
B2; occ.; U_{iso}		2c (1/3,2/3,0); 1.00 B2; 0.024(49)
Residual density; max; min [el/nm^3]x1000	1.30; -1.04	3.808; -2.795

[a] crystal structure data are standardized using the program Structure Tidy [49], [b, c] anisotropic (U_{ij}) and isotropic (U_{iso}) atomic displacement parameters are given in [10 nm^2], [d] fixed parameter.

Table 2. Interatomic distances (in 10 nm) derived from single crystal X-ray diffraction data

$(Pt_{1-x}Cu_x)_3Cu_2B$ (x=0.33)	$Pt_9Cu_3B_5$	
M1[a] – 2 B1 2.1157(3)	Pt1 - B1 2.15(4)	Cu1 - Pt2 2.548(6)
4 M1 2.7267(4)	2 B2 2.196(2)	4 Pt1 2.675(4)
2 Cu1 2.729(1)	2 Cu1 2.675(4)	4 Pt1 2.783(5)
2 Cu1 2.748(1)	2 Cu1 2.783(5)	2 Cu1 2.909(1)
2 Cu1 2.801(1)	2 Pt1 2.849(2)	
2 M1 2.9983(5)	2 Pt2 2.877(2)	
	2 Pt1 2.909(1)	
	Pt1 3.084(2)	
Cu1- 3 Cu1 2.524(1)	Pt2 - 4 B1 2.23(3)	B1 - 2 Pt1 2.15(4)
3 M1 2.729(1)	Cu1 2.548(6)	4 Pt2 2.23(3)
3 M1 2.749(1)	2 Pt2 2.7609(9)	
3 M1 2.801(1)	4 Pt1 2.877(2)	
	2 Pt2 2.909(1)	
B1 - 6 M1 2.1157(3)		B2 - 6 Pt1 2.196(2)

[a] M1=0.670(4) Pt+0.330(4) Cu

such connectivity creates larger distorted channels exhibiting pentagonal cross sections which embed the Cu atoms, and smaller trigonal channels (around the vacant site 1*b* (0,0,½)) which remain unoccupied. Thus, every copper atom appears to be surrounded by nine Pt, eight of which form a distorted tetragonal prism (Pt1 in 6*k*: *x*,*y*, ½) while one (Pt2 in 3*f*: *x*,0,0) is centering one of the faces; two Cu atoms which are located above and below the central one complete the polyhedron around Cu. Pt1 and Pt2 has 3 boron, 4 copper, 7 platinum and 4 boron, 1 copper, 8 platinum neighbours respectively at average distances d_{Pt-B}=0.221 nm, d_{Pt-Cu}=0.2693 nm. These distances excellently agree with the sums of Pauling's single bond radii (Pt-B 0.220 nm, Pt-Cu 0.261 nm) [52]. The crystal structure of $Pt_9Cu_3B_5$ is depicted in Fig. 2a-d showing the coordination polyhedra for all atom sites.

3.3. $(Pt_{1-x}Cu_x)_3Cu_2B$: structural relationships and site preferences

The structure of cubic elemental *β*-Mn exhibits interstitials voids with the shapes of octahedra and tetrahedra [19]. There is a series of non-metallic filled *β*-Mn-type phases crystallizing in the space group *R*32, e.g. M_7Te_{10}, AM_6Te_{10}, $Ag_2Ga_6Te_{10}$, RbX_4I_5 (M=Al, Ga, In; A=Ca, Pb, Sn; X=Ag, Cu) [23,53,54]; in these structures different fractions of the tetrahedral and octahedral holes of the *β*-Mn like arrangement of nonmetal atoms are occupied by metal atoms or pairs of covalently bonded metal atoms. The $(Pt_{1-x}Cu_x)_3Cu_2B$ structure together with few other reported borides (Cr_2Re_3B [34], $W_7Re_{13}B$ and $Mo_7Re_{13}B$ [33], Li_2Pt_3B and Li_2Pd_3B [30]) belong to another family of filled *β*-Mn-type structures where only the octahedral voids formed by metal atoms are occupied by boron; this structural arrangement has long been known also for a relatively large number of nitrides and carbides [55-64].

Commonly the *β*-Mn-type derivative structures are discussed in terms of a three-dimensional framework of all vertex-sharing filled M_6 octahedra. An alternative presentation can be illustrated when viewing the $(Pt_{1-x}Cu_x)_3Cu_2B$ structure in trigonal setting along the *c* direction: it exhibits infinite columns formed by two face-sharing $[Cu1Cu_3(Pt/Cu)_9]$ icosahedra interleaved with $[B(Pt/Cu)_6]$ octahedra; those columns run infinitively along the *c* axis trough *x*=0 *y*=0, *x*=⅔ *y*=⅓, and *x*=⅓ *y*=⅔ (Fig. 1e).

According to structural studies reported recently on Mg_3Ru_2 [65] and $Zn_{12-x}Co_{8+x}$ [24], the elements exhibiting higher Pauling electronegativity [66], i. e. Ru and Co reside predominantly in the 8*c* position, while Mg and Zn with smaller electronegativity values fill the 12*d* site. In both structures, the atom site with smaller coordination number (8*c*) attracts the smaller atom, whereas Zn and Mg fill the majority 12*d* sites with CN 14. Similarly, the same tendency has been observed for the Mo_3Pt_2N and Mo_3Pd_2N nitrides exhibiting filled *β*-Mn-type structures [58,59] while in $(Pt_{1-x}Cu_x)_3Cu_2B$ as well as in reported ternary borides TM_3Li_2B (TM=Pd,Pt) [30] and Re_3Cr_2B [34], the less electronegative element according to

Pauling's scale prefers the 8*c* site and more electronegative elements reside in the 12*d* site. The larger metal atom in $(Pt_{1-x}Cu_x)_3Cu_2B$ occupies predominantly the atom site with the highest coordination number (12*d*, CN=14). The latter tendency which was encountered earlier also in the $Cr_{23}C_6$-type $(MM')_{23}B_6$ phases [17] holds for the majority of ternary *β*-Mn-type carbides and nitrides as well.

3.4. $Pt_9Cu_3B_5$: structural relationships

The prototype structure [41] is related to $LiPt_3B$ [67] which itself is described as a boron deficient shift variant of the $CeCo_3B_2$-type [68]. Accordingly, the crystal structure of $Pt_9Cu_3B_5$ features the columns of platinum trigonal prisms which are interlinked by common edges to form the channels accommodating Cu but only part of them exhibits the similarity with the $CeCo_3B_2$-type structure (namely two $[BPt_6]$ trigonal prisms with the prisms axes directed along *c* and coinciding with the direction of Cu atoms chains) while the remaining prisms are arranged perpendicularly to the *c* direction. Furthermore, two transition metal atoms of the hexagonal ring in the planar Kagome net 3.6.3.6 of the $CeCo_3B_2$ structure are replaced by one (Pt2 in 3*f* (*x*,0,0) *x*=0.1761) which itself is shifted by *c*/2, similar to the structure of $LiPt_3B$-type. Such distortion converts the $[CeCo_{12}]$ hexagonal prism of $CeCo_3B_2$ to a distorted tetragonal prism with an additional platinum atom $[CuPt_5]$ centering one of the faces in the $Pt_9Cu_3B_5$ structure and, as a consequence, leads to the formation of BPt_8 rhombic units composed of two trigonal prisms inter-connected via rectangular faces whereby one of the prisms is filled by boron (B1 in 3*g* (*x*,0,½)). Those prisms aggregate via common prisms edges around the trigonal-prismatic vacancy in 1*b* (0,0,½) (d_{-Pt}=0.216 nm, d_{-B}=0.171nm) to build a cluster composed of seven Pt_6 trigonal prisms, six of which are positioned perpendicularly to the central one. This cluster is located at the origin of the unit cell.

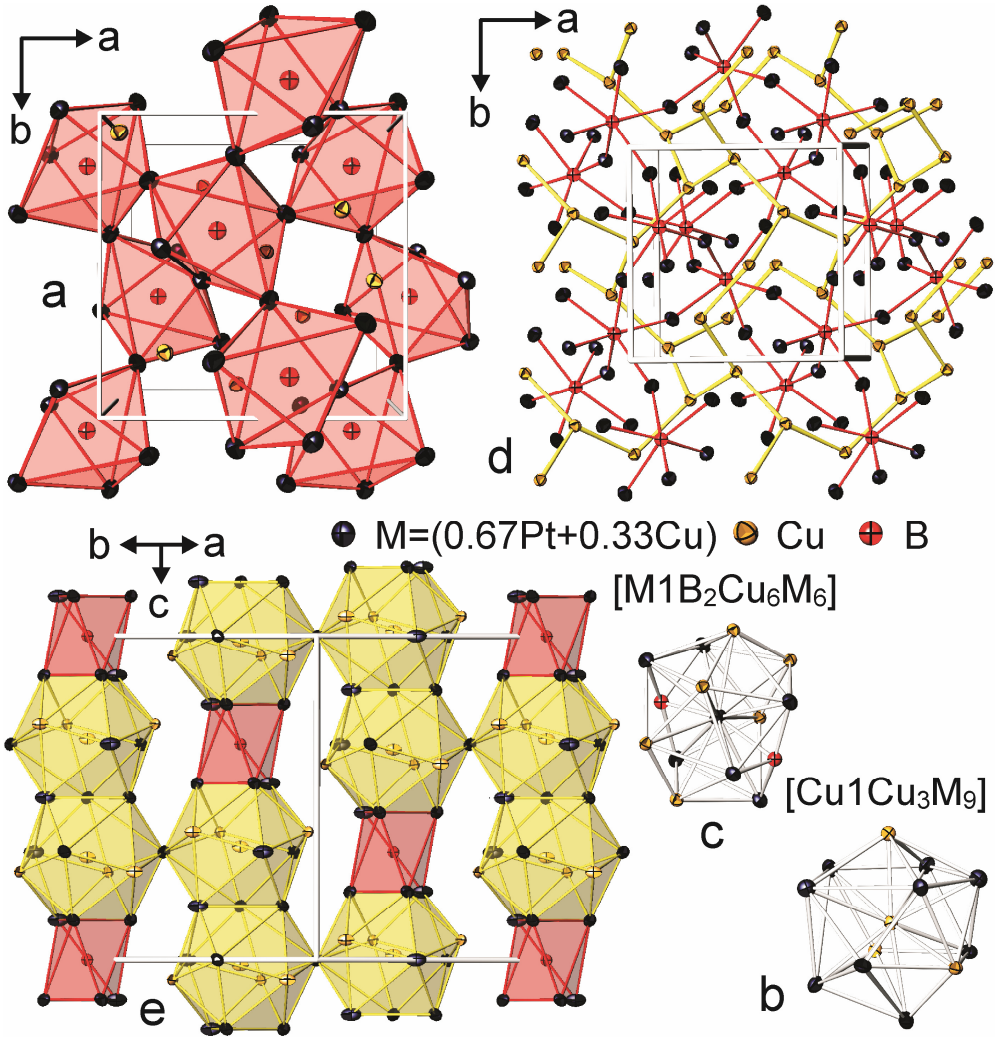

Fig. 1. Crystal structure of $(Pt_{1-x}Cu_x)_3Cu_2B$ showing a three dimensional connection of $[B(Pt/Cu)_6]$ octahedra (a). Coordination polyhedra of Cu and Pt/Cu (b-c). Interpenetrating Cu (yellow bonds) and $[B(Pt/Cu)_6]$ partial structures (red bonds) (white and black bonds correspondingly in black/white version) (d). Columns of $[Cu1Cu_3(Pt/Cu)_9]$ icosahedra and $[B(Pt/Cu)_6]$ octahedra running along 3-fold axes (a (111) slab in trigonal setting) (e).

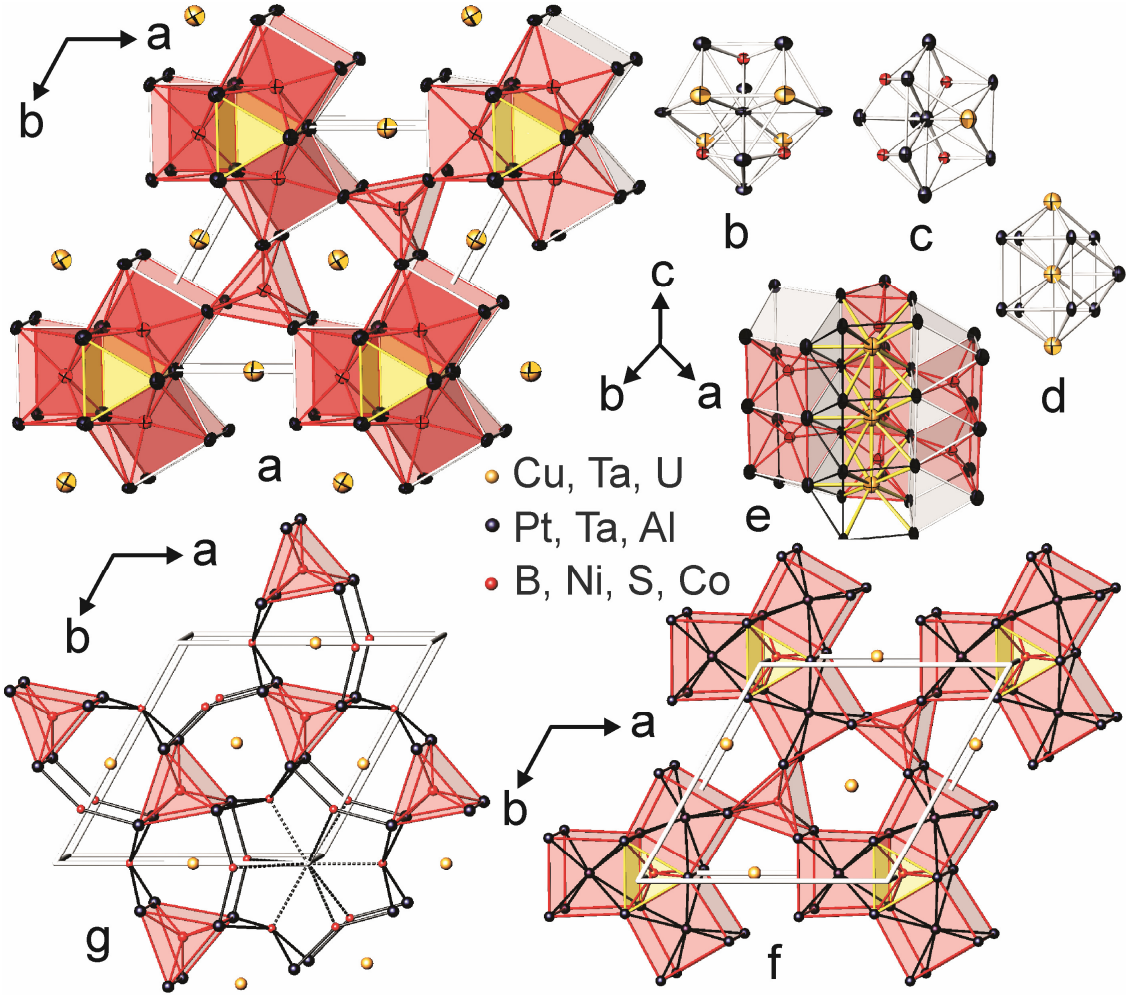

Fig. 2. Crystal structure of $Pt_9Cu_3B_5$ viewed along *c* direction outlining the columns of boron filled (red) and empty (yellow and white) Pt_6 trigonal prisms (light grey, and dark grey and white in black-and-white version correspondingly) (a). $[Pt1B_3Cu_4Pt_7]$ (b), $[Pt2B_4Cu_1Pt_8]$ (c) and $[Cu1Cu_2Pt_9]$ (d) coordination polyhedra. Enlarged view of columns of boron-filled and empty trigonal prisms (e). Unit cell of $UCoAl_4$ showing the near-neighbouring atoms of Co1 and Al3 ($[CoAl_6]$ and $[AlCo_8]$ respectively, both in red colour (light grey colour in black-and-white version) and Co2 ($[CoAl_6]$ in yellow (dark grey) colour) (f). Projection of the $Ta_9Ni_2S_6$ structure appr. along *c* direction with emphasis of the Ta_6 trigonal prisms around Ni and the nearest atom environment of the empty 1*b* (0,0,½) site (dashed lines) (g).

Considering the interatomic distances, the trigonal prismatic voids at the origin of the unit cell in the structure of $Pt_9Cu_3B_5$ offer sufficient spatial conditions to host a small atom like B, C, *etc,* as was confirmed recently in the boride structure with the general formula $Ti_{1+x}Os_{2-x}RuB_2$ (space group *P*-62*m*; *a*=0.88554 nm, *c*=0.30336 nm, Os/Ti in 6*k*, *x*=0.1883, *y*=0.46384, *z*=½; Ru in 3*f*, *x*=0.1736, *y*=0, *z*=0; Ti/Os in 3*f*, *x*=0.5810; *y*=0, *z*=0; B in 1*b*, *x*=0, *y*=0, *z*=½; B in 3*g*, *x*=0.7870, *y*=0, *z*=½; B in 2*c* *x*=⅓, y=⅔, *z*=0, origin in 0,0,0) [42,43]. Insertion of a boron atom into the empty site 1*b* (0,0,½) of $Pt_9Cu_3B_5$ would lead to the formation of trigonal-planar B_4 units.

The columnar structural blocks encountered in $Pt_9Cu_3B_5$ are frequently considered as the fundamental unit for a large number of layered structures [69] including those which are built of $MgCuAl_2$-type [70] slabs (ordered Re_3B-type [71]) intergrown with M-rich slabs having other structures and which have been discussed on a much broader basis elsewhere [72,73]. The detailed view into aluminide systems revealed a compound which is related to the $Pt_9Cu_3B_5$ structure in the system U-Co-Al (Fig. 2f), i.e. the $UCoAl_4$ [74], space group *P*-62*m*, *a*=0.9161 nm, *c*=0.41114 nm. Comparing both structures, one can see that U occupies the atom position of Cu, whereas Co1 and Al1 are situated in the atom site of B2 and Pt1, respectively. Both Al2 and Al3 atoms in $UCoAl_4$ are shifted by *c*/2 with respect to Pt2 and B1 in $Pt_9Cu_3B_5$ thereby maintaining planar heptagonal Al_5 rings of the $MgCuAl_2$-type as well as converting two trigonal prisms ([BPt_6] and [Pt_6]) of $Pt_9Cu_3B_5$ coupled by rectangular faces and positioned perpendicularly to the short axis into distorted squared prisms [$Al3Al_8$]. Co2 occupies the 2*c* atom site inside the trigonal prism [$Co2Al_6$] which is empty in the $Pt_9Cu_3B_5$ structure.

The analysis of the hitherto known chalcogenides revealed the correspondence of the geometry of the $Pt_9Cu_3B_5$ with the structure of $Ta_9Ni_2S_6$ [75,76] (Fig. 2g) (space group *P*-62*m*, *a*=1.0127 nm, *c*=0.3367 nm) where Ta2 (6*k*, *x*=0.1968, *y*=0.4603, *z*=½) and S2 (3*f*,

x=0.2953, *y*=0, *z*=0) build the heptagonal channels (formed by atom sites which correspond to Pt1 and Pt2) along the *c* axis, accommodating chains of Ta1 (in 3*f*, *x*=0.5466, *y*=0, *z*=0) (Cu1 site in $Cu_3Pt_9B_5$), and Ni takes the 2*c* (⅓,⅔,0) site of B2. Both sulfur sites are bridging the [$NiTa_6$] trigonal prisms. The atom position of S1 (3*g*, *x*=0.7316, *y*=0, *z*=½) corresponds to that of B1, however, exhibits a significant shift along *a* towards Ta1. This pronounced movement of S1 explains the existence of a larger channel ($d_{\text{-S}}$ = 0.301 nm and 0.319 nm in comparison with $d_{\text{-B}}$ = 0.171nm in $Pt_9Cu_3B_5$) running along the *z* axis through the origin of the structure of $Ta_9Ni_2S_6$.

3.5. Physical properties

Considering the elemental composition of the compounds investigated in this work, a simple metallic behavior without any magnetic phase transitions is expected.

A least-square fit (Fig. 3a) using the Bloch-Grüneisen relation

$$\rho = \rho_0 + C\frac{T^5}{\theta_D{}^6}\int_0^{\theta_D/T}\frac{x^5}{(e^x-1)(1-e^{-x})}dx \qquad (1)$$

was applied to $Pt_9Cu_3B_5$ ($Pt_9Zn_3B_{5-\delta}$-type structure) thereby revealing the Debye temperature $\theta_D = 203$ K and the residual resistivity $\rho_0 = 5.85\,\mu\Omega*\text{cm}$.

Measurements of the temperature dependent electrical resistivity carried out on a newly prepared single-phase sample $(Pt_{1-x}Cu_x)_3Cu_2B$ (where x=0.3 according to the results of Rietveld refinement of X-ray powder diffraction data; B-filled *β*-Mn-type structure) in the high temperature region clearly evidenced metallic behaviour. A rather high residual resistivity and, correspondingly a small residual resistivity ratio (RRR = 1.04) evidences a substantial concentration of scattering centers in this sample (Fig. 3b). Besides, a pronounced curvature in $\rho(T)$ is found for temperatures above about 70 K. A drop of the resistivity to zero below $T \approx 2\,\text{K}$ characterizes $(Pt_{1-3}Cu_x)_3Cu_2B$ as a novel superconductor.

The Bloch-Grüneisen relation was found to be not appropriate to describe the behaviour of the electrical resistivity of $(Pt_{1-x}Cu_x)_3Cu_2B$ (Fig. 3b) in the high temperature region; rather, the parallel resistance model was used,

$$\frac{1}{\rho} = \frac{1}{\rho_{ideal}} + \frac{1}{\rho_{sat}} \qquad (2)$$

where ρ_{ideal} corresponds to a Bloch-Grüneisen relation (Eqn. 1), revealing $\theta_D = 123$ K and a saturating resistance $\rho_{sat} = 145\ \mu\Omega * \mathrm{cm}$. The low value of the Debye temperature derived here might refer to a rather soft lattice, a promising initial situation for superconductivity.

The inset of Fig. 3b shows the dependence of the electrical resistivity of $(Pt_{1-x}Cu_x)_3Cu_2B$ on externally applied magnetic fields. As expected for superconductors, the increase of applied magnetic fields decreases the superconducting transition temperature until the transition is completely suppressed around 2T. Using the data displayed in Figure 3b, the temperature dependence of the upper critical magnetic field $\mu_0 H_{C2}(T)$ is constructed and presented in Fig. 4.

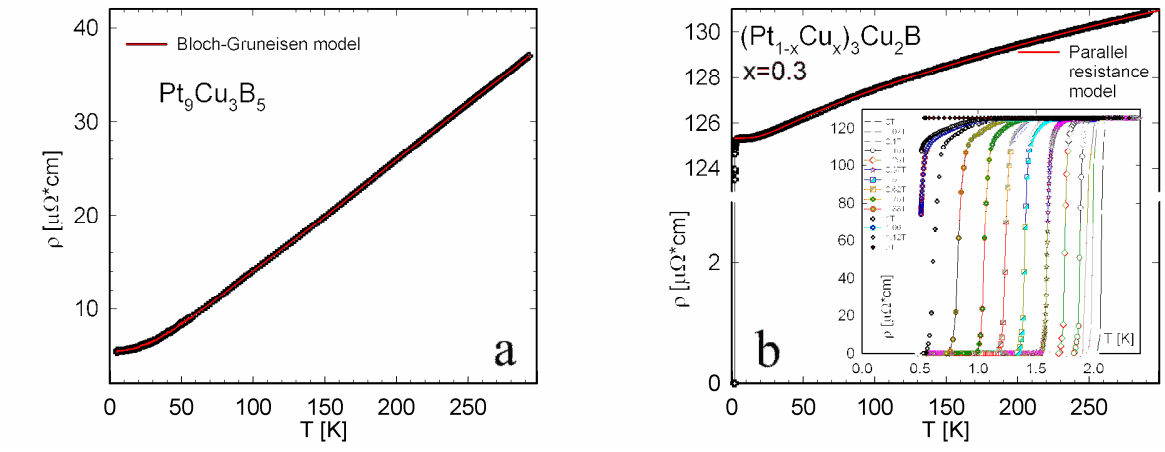

Fig. 3. (a) Temperature dependent electrical resistivity of $Pt_9Cu_3B_5$. The solid line is a least square fit according to Eqn. 1. (b) Temperature dependent electrical resistivity of $(Pt_{1-x}Cu_x)_3Cu_2B$. The solid line is a least square fit according to Eqn. 2. The inset describes the evolution of the electrical resistivity under the influence of magnetic fields.

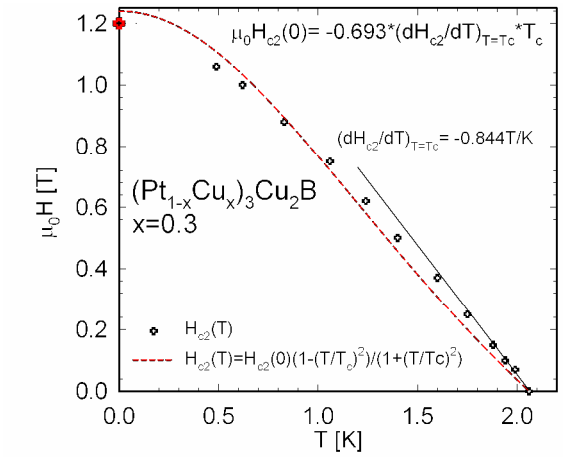

Fig. 4. Temperature dependent upper critical field $\mu_0 H_{C2}$ of $(Pt_{1-x}Cu_x)_3Cu_2B$. Dashed line is explained in the text.

We estimate the $\mu_0 H_{C2}(0)$ from the Werthamer-Helfand-Hohenberg (WHH) model [77] as

$$\mu_0 H_{C2}(0) = -0.693\left(dH_{C2}/dT\right)_{T=T_C} T_C = 1.2\ \mathrm{T},$$

a value which is in a good agreement with the experimental data. A least-square fit (dashed line) using a semi-empirical model

$$H_{C2}(T) = H_{C2}(0)\left(1-(T/T_C)^2\right)/\left(1+(T/T_C)^2\right)$$

lead to a slightly higher value of upper critical field of $\mu_0 H_{C2}(0) = 1.24\,\mathrm{T}$.

Preliminary ac susceptibility measurements reveal ideal diamagnetism of the full sample volume and specific heat data display a reasonably large superconducting anomaly, thus, confirming the bulk nature of superconductivity in $(Pt_{1-x}Cu_x)_3Cu_2B$.

4. Conclusions

In conclusion, we have synthesized for the first time and characterized by X-ray single crystal and powder diffraction two copper platinum borides, $(Pt_{1-x}Cu_x)_3Cu_2B$ (x=0.33) and $Pt_9Cu_3B_5$.

$(Pt_{1-x}Cu_x)_3Cu_2B$ (x=0.33) is a new member of the filled *β*-Mn structure where boron atoms are located inside octahedral clusters formed by metal (Pt/Cu) atoms, while the net-like copper atoms sub-lattice interlace with $[B(Pt/Cu)_6]$ octahedra. Different branches of the *β*-Mn-type family tree have been considered, however the structure refinement of X-ray single crystal data confirmed the higher symmetric $P4_132$ space group leaving no arguments for a symmetry reduction. Atomic site occupancies follow the tendency observed for the majority of *β*-Mn-type related borides.

Despite the formulae of $Pt_9Cu_3B_5$ (isotypic with $Pt_9Zn_3B_{5-\delta}$) is close to that of borides of a ternary ordered variant of the $CaCu_5$-type, the structure does not exhibit M atoms in planar Kagome nets (3.6.3.6) perpendicular to [001] and alternating along the short translation vector with layers of M and B atoms. The peculiar platinum nets are modified to form puckered pentagons, distorted rectangles and triangles. Boron interacts exclusively with Pt but Cu is located within channels infinitively extending along *z* with a pentagonal cross section. Both boron atoms have trigonal prismatic coordination $[BPt_6]$. There are also empty $[Pt_6]$ trigonal prisms located at the origin of the unit cell which are able to accommodate additional boron atoms and if so, would form B_4 planar units with surrounding boron atoms similar to the $Ti_{1+x}Os_{2-x}RuB_2$ structure. All trigonal prisms are arranged to build columns running along the *c* direction. B filled trigonal prisms from different columns have axes which are perpendicular to each other. The comparison of $Pt_9Cu_3B_5$ with aluminide and chalcogenide structures revealed the geometrical relationships with $UCoAl_4$ and $Ta_9Ni_2S_6$.

$Pt_9Cu_3B_5$ ($Pt_9Zn_3B_{5-\delta}$-type structure) exhibits a metallic type of temperature dependence for electrical resistivity, while the $(Pt_{1-x}Cu_x)_3Cu_2B$ (B-filled *β*-Mn-type structure) shows a sharp superconducting transition at 2.06 K. From analysis of literature data on the electrical resistivity behavior of the isotypic compounds complemented by the current study

one may assume that the filled β-Mn-type structure favors the occurrence of superconductivity in ternary borides.

Acknowledgement

The research work of O.S. was supported by Austrian FWF project V279-N19. Authors are very thankful to Dr. Klaudia Hradil (XRC TU Wien) for collaboration and to Mrs. Monika Waas for SEM measurements.

Supporting Information

Supplementary data associated with this article (Rietveld X-ray powder diffraction refinement of $(Pt_{1-x}Cu_x)_3Cu_2B$ (x=0.3)) can be found in the online version at ….

References

[1] Z. Zachary, New superhard ternary borides in composite materials, In New Superhard Ternary Borides in Composite Materials, Metal, Ceramic and Polymeric Composites for Various Uses, Cuppoletti, J., Ed, Int. Tech, 2011, 61–78. and the references herein

[2] K. Takagi, M. Komai, T. Ide, T. Watanabe, Y. Kondo, Int. J. Powder Metall. 23 (1987) 157-163.

[3] W. Yongguo, L. Zhaoqian, Mat. Res. Bul. 67 (2001) 417-423.

[4] H.-Y. Chung, M.B. Weinberger, J.B. Levine, A. Kavner, J.-M. Yang, S.H. Tolbert, R.B. Kaner, Science 316 (2007) 436-439.

[5] J. Nagamatsu, N. Nakagawa, T. Muranaka, Yu. Zenitani, J. Akimitsu, Nature 410 (2001) 63-64.

[6] E.Y. Zarechnaya, L. Dubrovinsky, N. Dubrovinskaia, N. Miyajima, Y. Filinchuk, D. Chernyshov, V. Dmitriev, Sci. Tech. Adv. Mat. 9 (2008) 044209-4.

[7] E.Y. Zarechnaya, L. Dubrovinsky, N. Dubrovinskaia, Y. Filinchuk, D. Chernyshov, V. Dmitriev, N. Miyajima, A. El Goresy, H.F. Braun, S. Vansmaalen, I. Kantor, A. Kantor, V. Prakapenka, M. Hanfland, A.S. Mikhailushkin, I.A. Abrikosov, S.I. Simak, Phys. Rev. Lett. 102 (2009) 185501-4.

[8] J.B. Levine, S.H. Tolbert, R.B. Kaner, Adv. Funct. Mater. 19 (2009) 3519–3533.

[9] B.P.T. Fokwa, Borides: Solid-State Chemistry, Encyclopedia of Inorganic and Bioinorganic Chemistry, 2014, ed R.A. Scott, John Wiley: Chichester, John Wiley & Sons, Ltd. and the references herein.

[10] D. Kotzott, M. Ade, H. Hillebrecht, J. Solid State Chem. 183 (2010) 2281-2289.

[11] J. Brgoch, C. Goerens, B.P.T. Fokwa, G.J. Miller, J. Am. Chem. Soc. 133 (17) (2011) 6832-6840.

[12] B.P.T. Fokwa, H. Lueken, R. Dronskowski, Chem. Eur. J. 13(21) (2007) 6040-6046.

[13] V.L. Deringer, Ch. Goerens, M. Esters, R. Dronskowski, B.P.T. Fokwa, Inorg. Chem. 51(10) (2012) 5677-5685.

[14] M. Mbarki, R.St. Touzani, B.P.T. Fokwa, J. Solid State Chem. 203 (2013) 304-309.

[15] M. Hermus, B.P.T. Fokwa, J. Solid State Chem. 183(4) (2010) 784-788.

[16] B.P.T. Fokwa, R. Dronskowski, Z. Anorg. Allg. Chem. 634 (2008), 1955-1960.

[17] O. Sologub, P. Rogl, Giester G. Intermetallics 18 (2010) 694–701.

[18] C.B. Shoemaker, D.P. Shoemaker, T.E. Hopkins, S. Yindepit, Acta Crystallogr. B 34 (1978) 3573-3576.

[19] P.I. Kripyakevich, Zh. Strukt. Khim. 1963, 4(1), 118-136; Zh. Strukt. Khim. 4(2) (1963) 282-299.

[20] M. O'Keeffe, S. Anderson, Acta Crystallogr. A33 (1977) 914-923.

[21] H. Nyman, C.E. Carroll, B.G. Hyde, Z. Kristallogr. 196 (1991) 39-46.

[22] O. B. Karlsen, A. Kjekshus, C. Rømming, E. Røst, Acta Chem. Scand. 46 (1992) 1076-1082.

[23] H.J. Deiseroth, H.D. Muller, Z. Anorg. Allg. Chem. 622 (1996) 405-420.

[24] W. Xie, S. Thimmaiah, J. Lamsal, J. Liu, T.W. Heitmann, D. Quirinale, A.I. Goldman, V. Pecharsky, G.J. Miller, Inorg. Chem. 52 (2013) 9399–9408.

[25] W. Jeitschko, H. Nowotny, F. Benesovsky, Monatsh. Chem. 94 (1963) 247-251.

[26] J. Johnston, L. Toth, K. Kennedy, E.R. Parker, Solid State Comm. 2 (1964) 123.

[27] E. Bauer, G. Rogl, X.-Q. Chen, R.T. Khan, H. Michor, G. Hilscher, E. Royanian, K. Kumagai, D.Z. Li, Y.Y. Li, R. Podloucky, P. Rogl, Phys. Rev. B 82 (2010) 064511-5.

[28] A.B. Karki, Y.M. Xiong, I. Vekhter, D. Browne, P.W. Adams, D.P. Young, K.R. Thomas, Ju.Y. Chan, H. Kim, R. Prozorov, Phys. Rev. B 82 (2010) 064512-7.

[29] E. Bauer, C. Sekine, U. Sai, P. Rogl, P.K. Biswas, A. Amato, Phys. Rev. B 90 (2014) 054522-5.

[30] U. Eibenstein, W. Jung, J. Solid State Chem. 133 (1997) 21-24.

[31] K. Togano, P. Badica, Y. Nakamori, S. Orimo, H. Takeya, K. Hirata, Phys. Rev. Lett. 93 (2004) 247004-4.

[32] H.Q. Yuan, D.F. Agterberg, N. Hayashi, P. Badica, D. Vandervelde, K. Togano, M. Sigrist, M.B. Salamon, Phys. Rev. Lett. 97 (2006) 017006-4.

[33] K. Kawashima, A. Kawano, T. Muranaka, J. Akimitsu, J. Phys. Soc. Jpn. 74 (2005) 700-704.

[34] H. Niimura, K. Kawashima, K. Inoue, M. Yoshikawa, J. Akimitsu, J. Phys. Soc. Jpn. 83 (2014) 044702-5.

[35] O. Sologub, P. Rogl, E. Bauer, L. Salamakha, A. Gonçalves, C. Rizzoli, G. Giester, H. Noël, Ternary Ytterbium-Platinum-Boron and related systems with Sc and Y. A contribution to the structural chemistry of the binary platinum borides, Conference Abstract, SCTE 2014-19th International Conference on Solid Compounds of Transition Elements, 21-26 June 2014, Genova-Italy, Book of Abstracts, p. 109

[36] L. Salamakha, E. Bauer, G. Hilscher, H. Michor, O. Sologub, P. Rogl, G. Giester, Inorg. Chem. 2013, 52 (8) (2013) 4185–4197.

[37] O.L. Sologub, J.R. Hester, P.S. Salamakha, E. Lerroy, C. Godart, J. Alloys Comp. 337 (2002) 10-17.

[38] O. Sologub, P. Salamakha, H. Noel, M. Potel, M. Almeida, C. Godart, J. Alloys Comp. 307 (2000) 40-44.

[39] U. Eibenstein, W. Klünter, W. Z. Jung, Anorg. Allg. Chem. 625 (1999) 719-724.

[40] K. Petry, W. Jung, J. Alloys Compd. 183 (1992) 363-376.

[41] K. Petry, W. Klünter, W. Jung, Z. Kristallogr. 209 (1994) 151-156.

[42] B.P.T. Fokwa, J. von Appen, R. Dronskowski, Chem. Commun. (2006) 4419–4421.

[43] V.L. Deringer, Ch. Goerens, M. Esters, R. Dronskowski, B.P.T. Fokwa, Inorg. Chem. 51 (2012) 5677–5685.

[44] J. Rodriguez-Carvajal, Physica B 192 (1993) 55-69.

[45] Bruker Advanced X-ray solutions. APEX2 User Manual. Version 1.22. 2004, Bruker AXS Inc.

[46] Bruker. APEXII, SAINT and SADABS. 2008, Bruker Analytical X-ray Instruments, Inc., Madison, Wisconsin, USA.

[47] G.M. Sheldrick, SHELXS-97, Program for the Solution of Crystal Structures; University of Göttingen, Germany, 1997.

[48] G.M. Sheldrick, SHELXL-97, Program for Crystal Structure Refinement; University of Göttingen, 1997.

[49] E. Parthé, L. Gelato, B. Chabot, M. Penzo, K. Censual, R. Gladyshevskii, TYPIX – Standardized Data and Crystal Chemical Characterization of Inorganic Structure Types; Berlin: Springer, 1994.

[50] P. McArdle, J. Appl. Cryst. 29 (1996) 306.

[51] L.J. J. Farrugia, J. Appl. Cryst. 32 (1999) 837-838.

[52] L. Pauling, B. Kamb, A revised set of values of single-bond radii derived from the observed interatomic distances in metals by correction for bond number and resonance energy Proc. Natl. Acad. Sci. USA 83 (1986) 3569-3571.

[53] R. Nesper, J. Curda, Z. Naturforsch. 42b (1987) 557-564.

[54] H.J. Deiseroth, H.-D. Müller, Z. Kristallogr. 210 (1995) 57-58.

[55] T.J. Prior, P.D. Battle, J. Solid State Chem. 172 (2003) 138–147.

[56] T.J. Prior, D. Nguyen-Manh, V.J. Couper, P.D. Battle J. Phys.: Condens. Matter 16 (2004) 2273-2281.

[57] K.S. Weil, P.N. Kumta, J. Grins, J. Solid State Chem. 146 (1999) 22-35.

[58] A. El Himri, F. Sapina, R. Ibanez, A. Beltran, J. Mater. Chem. 11 (2001) 2311-2314.

[59] A. El Himri, D. Marrero Lopez, P. Nunez, J. Solid State Chem. 177 (2004) 3219-3223.

[60] D. Errandonea, C. Ferrer-Roca, D. Martinez-Garcia, A. Segura, O. Gomis, A. Munoz, P. Rodriguez-Hernandez, J. Lopez-Solano, S. Alconchel, F. Sapina, Phys. Rev. B 82 (2010) 174105-8.

[61] P. Subramanya Herle, M.S. Hegde, K. Sooryanarayana, T.N. Guru Row, G.N. Subbanna, J. Mater. Chem. 8(6) (1998) 1435–1440.

[62] W. Jeitschko, H. Nowotny, F. Benesovsky, Monatsh. Chem. 94 (1963) 332-333.

[63] H.J. Goldschmidt, Metallurgia 56 (1957) 17–26.

[64] A.C. Lawson, J. Less-Common Met. 23 (1971) 103-106.

[65] R. Pottgen, V. Hlukhyy, A. Baranov, Y. Grin, Inorg. Chem. 47 (2008) 6051-6055.

[66] L. Pauling, J. Am. Chem. Soc. 54 (1932) 3570-3582.

[67] R. Mirgel, W. Jung, J. Less-Common Met. 144 (1988) 87-99.

[68] Yu.B. Kuz'ma, P.I. Krypyakevych, N.S. Bilonizhko, Dopov. Akad. Nauk Ukr. RSR (Ser. A) (1969) 939-941.

[69] E. Parthe, B. Chabot, Crystal structures and crystal chemistry of ternary rare-earth transition metal borides, silicides and homologues, Handbook on the Physics and Chemistry of Rare Earths, eds K.A. Gschneidner Jr and L. Eyring Vol. 6, North-Holland, Amsterdam 1984, 113–334.

[70] H. Perlitz, A. Westgren, Ark. Kemi Mineral. Geol. 16B (1943) 13-1.

[71] B. Aronsson, M. Bäckman, S. Rundqvist, Acta Chem. Scand. 14 (1960) 1001-1005.

[72] R. Pottgen, M. Lukachuk, R.-D. Hoffmann, Z. Kristallogr. 221 (2006) 435–444.

[73] K.W. Richter, Yu. Prots, Yu. Grin, Inorg. Chem. 44(13) (2005) 4576-5485.

[74] J. Stepien-Damm, O. Tougait, V.I. Zaremba, H. Noël, R. Troc, Acta Cryst. C60 (2004) i7-i8.

[75] B. Harbrecht, H.F. Franzen, J. Less-Common Met. 113(2) (1985) 349–360.

[76] M.J. Calhorda, R. Hoffmann, Inorg. Chem. 27 (1988) 4679-468.

[77] N.R. Werthamer, E. Helfand, P.C. Hohenberg, Phys. Rev. 147 (1966) 295-302.